A Fundamental Verification of a Single-phase to Three-phase Matrix Converter with a PDM Control based on Space Vector Modulation

Yuki Nakata and Jun-ichi Itoh
Department of Electrical, Electronics and Information Engineering
Nagaoka University of Technology
Nagaoka, Niigata, Japan
nakata@nagaokaut.ac.jp, itoh@stn.nagokaut.ac.jp

***Abstract*—This paper discusses pulse density modulation (PDM) control methods for a single-phase to three-phase matrix converter for high-frequency applications such as the grid interface converter for a wireless power transfer system and high-frequency transformer link system. The input frequency for this converter is assumed as several hundred kHz, and at the same time outputting a commercial frequency, i.e. 50 Hz or 60 Hz. The proposed circuit achieves high efficiency by zero voltage switching from a PDM control method. In the PDM control using delta-sigma conversion, the output waveform has inverse voltage pulse and clamp phenomena on the output voltage waveform. Hence, an improvement method of the output waveform based on SVM is proposed. In this paper, the experimental results using the prototype circuit of indirect matrix converter (IMC) and conventional matrix converter (CMC) with the two PDM control methods are compared. As a result, the THD of the output voltage with delta-sigma conversion and PDM pattern method based on SVM are 5.96% and 2.15% respectively in the experiment using IMC. Furthermore, the maximum efficiency has been improved from 93.4% to 97.3% by applying the proposed PDM method. From the results, the validity of PDM control based on SVM has been confirmed. In addition, a prototype of direct type circuit (CMC) has been built and tested. From the results, the switching at zero voltage and clear sinusoidal output waveform has been confirmed too. As a result, the output voltage THD, which is controlled by the proposed PDM based on SVM are 3.25%.**

Keywords— delta-sigma conversion, PDM control, space vector modulation, wireless power transfer

I. INTRODUCTION

In recent years, wireless power transfer systems have been actively researched [1-4]. In the wireless power transfer system, the frequency of the generated voltage at the receiving coil is from tens of kHz to several MHz, which is identical to the power source frequency. Accordingly, in order to connect this system to a load, an interface converter which converts the received power into a controlled output power is required. The characteristic of this interface converter must have a high input frequency (several hundred kHz) and a low output frequency (50 Hz or 60 Hz) which is suitable for commercial power grid. That is, an AC-to-AC converter is generally clarified as the interface converter for this system. In general, back-to-back (BTB) system, which is constructed by a PWM rectifier, a smoothing capacitor and a PWM inverter, is used as this AC-to-AC converter. However, it is difficult to use the PWM rectifier in the input side due to high-frequency input.

On the other hand, matrix converters (MC) have been attracted attentions as the AC interface converter for the wireless system, because it delivers advantages in terms of a size reduction and an energy saving owning to high efficiency [5-7]. However, the implementation of the MC in the high-frequency power source has not been reported.

There are two type topologies for the matrix converter, so called indirect matrix converter (IMC) and conventional matrix converter (CMC). The IMC consists of a diode rectifier and three-phase inverter, and the configuration and the control of the circuit are simpler than the CMC circuit. However, the IMC has low efficiency because of the twice power conversion. Furthermore, the IMC circuit is a unidirectional power flow converter because the diode rectifier is used in the input side. On the other hand, the CMC consists of bidirectional switches. The CMC has high efficiency because of the only once power conversion. Additionally, this circuit is a bidirectional power flow converter because the bidirectional switches are used. However, control of this circuit is more complicated in comparison than that of the IMC because the input voltage polarity of the circuit alternates.

The authors have previously proposed a Pulse density modulation (PDM) [8-11] control method for the high-frequency power source [12-13]. The proposed PDM control method is applied to the proposed circuit by using the half cycle of the input voltage as a pulse for PDM control. Therefore the proposed circuit achieves the reduction of the switching loss by the switching at zero input voltage. The PDM signals can be obtained from delta-sigma conversion. However, in the delta-sigma conversion, the inverse voltage pulses and clamp phenomena occur in the output voltage waveform of the IMC. When the phase angle between the output voltage

and current becomes larger instantaneously, the DC link current flow backward to the power source and DC link voltage is clamp to snubber capacitor voltage because the DC link current cannot flow toward the power source. Therefore the clamp phenomenon of the output voltage occurs. Additionally, in CMC circuit, the clam phenomenon does not occur because the power regeneration is allowed in the CMC.

In this paper, the PDM control based on space vector modulation (SVM) is proposed in order to solve these problems and improve the quality of output waveform. The proposed method generates switching patterns based on SVM in order to minimize the phase angle between output voltage and current. Therefore, there are no clamp phenomena on the output voltage waveform of the IMC. This paper compares and investigates the two PDM control methods, which are based on the delta-sigma conversion and SVM are compared and investigated from the experimental results using the prototype circuit of IMC and CMC. Firstly, the configurations of the proposed circuit are introduced. Secondly, the PDM control strategy using the delta-sigma conversion and the proposed PDM method based on the SVM are discussed. Next, the validity of the proposed method is confirmed in the experimental results using the prototype circuit of IMC. Finally, the proposed PDM control method is applied to a prototype circuit of CMC, and the basic operation of the proposed PDM control in direct type circuit is confirmed.

II. CIRCUIT CONFIGURATION

A. System Configuration

Fig. 1 shows a configuration of the wireless power transfer system. The receiving coil voltage is a high-frequency AC, which has same as the frequency of the source. In order to connect to the commercial grid, a single phase AC to three phase AC converter is required as an interface converter.

The interface converter inputs several-hundred-kHz sinusoidal waveform, and outputs the low-frequency waveform such as 50 Hz and 60 Hz. Hence, PDM control which uses a half cycle of the input voltage as a pulse can be applied to the interface converter.

Therefore, the use of the matrix converter as an interface converter for wireless power transfer system is proposed. The matrix converter has high frequency by applying proposed PDM control. The detail of PDM control is explained in next section.

B. Indirect Single-phase to Three-phase Matrix Converter

Fig. 2 shows circuit configuration of the proposed single-phase to three-phase IMC. This circuit is constructed from a diode rectifier as an input interface and a three-phase inverter for the rear side. Since this converter does not required electrolytic capacitors in the DC link, the lifetime is longer and the size is more compact than the conventional system, which is

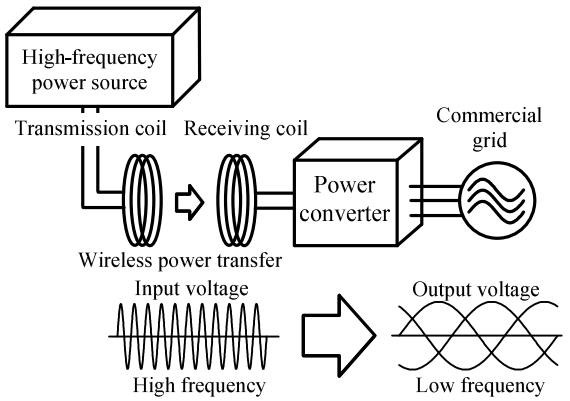

Fig. 1. Configuration of the wireless power transfer system.

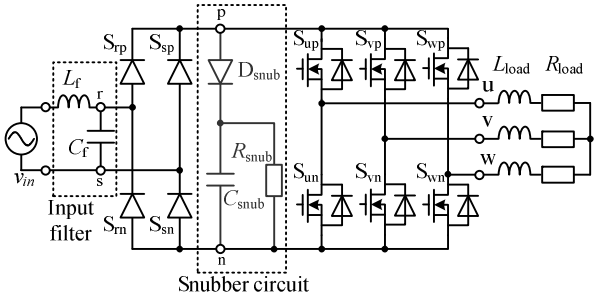

Fig. 2. Single-phase to three-phase indirect matrix converter.

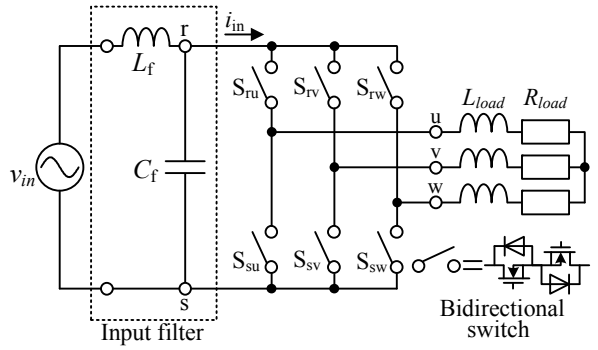

Fig. 3. Single-phase to three-phase conventional matrix converter.

constructed by a PWM rectifier, electrolytic capacitors and a three-phase PWM inverter.

The IMC has low efficiency because the power conversion number of the IMC is twice. Furthermore, the IMC circuit is a unidirectional power flow converter because the diode rectifier is used in the input side. However, the control of the circuit are simpler than the CMC circuit because the inverter is controlled only.

Note that, in the experimental circuit, a snubber circuit is connected to the DC link as a protection circuit. It is constructed by a diode, a small capacitor and a resistor.

The prototype of this circuit configuration is used in the first experiment, in order to compare two PDM methods, which is explained in chapter III and confirm the validity of the proposed method explained in section III-C.

C. Single-phase to Three-phase Matrix Converter

Fig. 3 shows the circuit configuration of the proposed single-phase to three-phase CMC. This circuit is

constructed by six bidirectional switches. Since this converter does not require electrolytic capacitors in the DC link, the lifetime is longer and the size is more compact than that of the conventional system, which is constructed by a PWM rectifier, electrolytic capacitors and a three-phase PWM inverter. Further, the efficiency of a CMC is higher than a conventional system because the conversion number is reduced in comparison with the conventional system. However, control of this circuit is more complicated in comparison than that of the IMC because the input voltage polarity of the circuit alternates.

Note that, in the experimental circuit, a snubber circuit is connected to the output side of the converter as a protection circuit. It is constructed by a diode, a small capacitor and a resistor.

The prototype of this circuit configuration is used in the second experiment, in order to confirm the basic operation and validity of proposed PDM method explained in section III-C in CMC.

D. Design of the Input Filter

The impedance matching is important on the circuit for the high-frequency application. In this system, the input filter is connected to the input side as an impedance matching circuit, which can match the impedance of the voltage source and the circuit. The design method, which matches the impedance Z_{in} to 50 Ω is explained in this section because the general high-frequency power sources have 50 Ω of matching impedance.

Fig. 4 shows the configuration of input filter. It is constructed from a reactor L_f and a capacitor C_f. The impedance of the load connected to the filter is expressed by resister R_{load} as shown in Fig. 4. The value of L_f and C_f are decided in order that the real part of the synthetic impedance equals to 50 Ω and the imaginary part equals to 0 Ω to achieve the 50 Ω of matching impedance. L_f and C_f are calculated by (1) and (2), where, $\omega=2\pi f$ is the input voltage angular frequency. L_f and C_f are 80 μH and 16 nF respectively, when the frequency of f is 100 kHz, and R_{load} is 100 Ω. These values are used in the experiment.

$$L_f = \frac{C_f {R_{load}}^2}{1+(\omega C_f R_{load})^2} \tag{1}$$

$$C_f = \frac{1}{\omega R_{load}}\sqrt{\frac{R_{load}}{50}-1} \tag{2}$$

III. CONTROL STRATEGYS

A. Concept of PDM Control

A PDM control method is applied to the proposed system in order to reduce the switching loss of the converter. PDM controls the density and the plus/minus of the constant-width pulse, and then these pulse signals are used as the output unit.

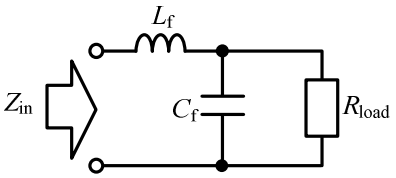

Fig. 4. Configuration of the input filter.

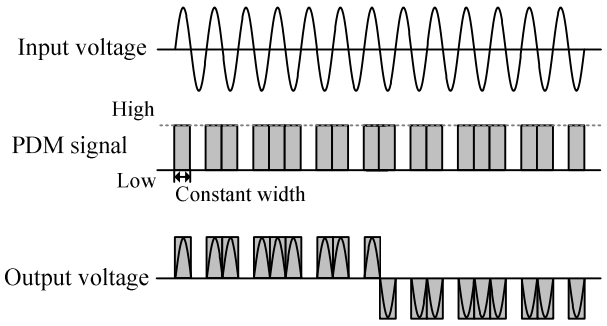

Fig. 5. PDM control waveform of proposed circuit.

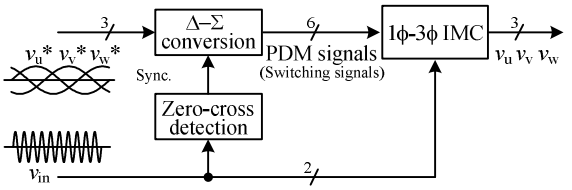

(a) Control block diagram using delta-sigma conversion (overall).

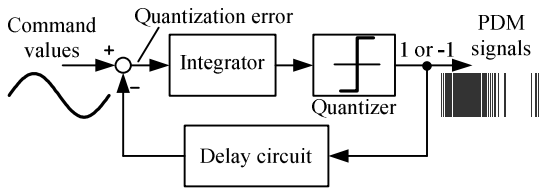

(b) Block diagram of the delta-sigma conversion.

Fig. 6. PDM control block diagram using delta-sigma conversion.

Fig. 5 shows a frame format of PDM control waveform for the single-phase to three-phase CMC. Assuming that the single-phase to three-phase CMC is connecting to a wireless power transfer system, it is receiving high frequency sinusoidal voltage as an input. Therefore the PDM control can be applied to the proposed circuit by using the half cycle of the input voltage as a pulse for PDM control as shown in Fig. 5.

B. PDM Control using Delta-sigma Conversion

Fig. 6 shows the PDM control block diagram using delta-sigma conversion. The PDM signals used for the switching can be obtained by applying the delta-sigma conversion to each phase command values (v_u^*, v_v^*, v_w^*). In general, delta-sigma conversion is used for analog-digital conversion. These PDM signals are used to turn on/off the inverter arm of IMC shown in Fig. 2.

Additionally, the zero cross points exist with respects to the frequency since the input voltage is a sinusoidal waveform. The turn-on and off of the each switching devices are implemented at every zero cross points of the input voltage in order to achieve the switching at zero

voltage. The loss from the switching devices at the converter can reduce drastically because the switching loss can be decreased nearly to zero by the implementation of the switching at zero voltage.

However, there are problems in this method, due to the inverse voltage pulses and clamp phenomena that are constant voltage areas occur shown as Fig. 8. Delta-sigma conversion generates the inverse voltage pulses in order to cancel the quantization error shown in Fig. 5(b). In the clamped parts, switching loss increases because the switching at zero voltage cannot be achieved. The clamp phenomenon occurs because when the phase angle between the output voltage and current becomes larger than 30 degrees, the DC link current flows backward to the power source in the inverter side. As a result, the DC link voltage is equaled to the snubber capacitor voltage.

In order to resolve this problem, the PDM based on SVM is proposed to apply for the generator of PDM patterns. The detail of this method is explained in the next section.

C. PDM Control based on Space Vector Modulation

Fig. 7(a) shows the PDM signal generation block based on the SVM. The selected vector signals generated from the SVM is the input to the D flip flop (D-FF). The plus/minus detection signal from the input voltage is used to detect the zero cross points of input voltage, and this signal is an input to the CLK of the D-FF. The output of the D-FF, "Q" is synchronized at the edge of plus/minus signal, which is the zero cross point of the input voltage. After that, the switching signals which correspond to the vectors in Fig. 7(b), are generated from output signals of the D-FF using pattern table in Fig. 7(c). These signals are Switching signals for IMC shown in Fig. 2.

Furthermore, in order to apply this method to CMC shown in Fig. 3, the switching signals are exclusive NORed with the polarity of the input voltage, because it is necessary to exchange the switching signals of the upper arm and the lower arm depending on the polarity of the input voltage.

Therefore, the switching patterns generated by SVM are quantized by the pulse whose width is half cycle of the input voltage and the switching timing is synchronized with the zero cross point of the input voltage. As a result, this proposed method based on SVM can achieve switching at zero voltage.

IV. Experimental Results using Indirect Matrix Converter and Conventional Matrix Converter

In this chapter, a prototype circuit of IMC and CMC are built and tested in order to demonstrate the validity of the proposed PDM methods.

First, the single-phase to three-phase IMC was tested in the experiment with the two PDM control methods in section IV-A and IV-B. A high-frequency power source, where the matching impedance is 50 Ω is used as the input of the circuit in order to confirm the basic principle of the two PDM control methods. Table I shows the experimental conditions.

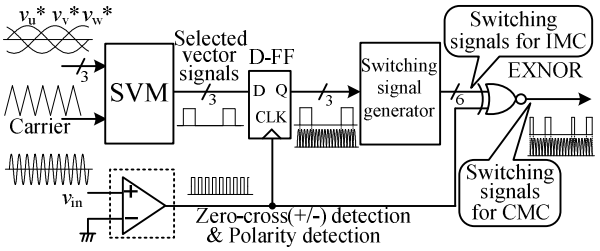

(a) PDM signals generation block diagram based on SVM.

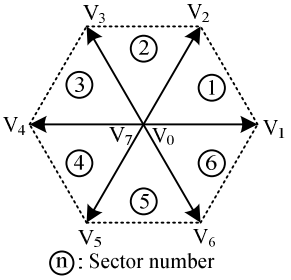

(b) Space vector diagram.

Selected Vector	Switching pattern		
	u	*v*	*w*
V_0	0	0	0
V_1	1	0	0
V_2	1	1	0
V_3	0	1	0
V_4	0	1	1
V_5	0	0	1
V_6	1	0	1
V_7	1	1	1

"1": ON, "0": OFF

(c) Switching pattern table.

Fig. 7. Control block diagram of the PDM control based on SVM

Table I. Experimental Parameters for IMC.

Parameter		Value
Input voltage		200 V
Input frequency		100 kHz
Output line-to-line voltage		100 V
Output frequency		50 Hz
Carrier frequency (in proposed PDM control based on SVM)		5 kHz
Load	R_{load}	100 Ω
	L_{load}	10 mH

Table II. Experimental Conditions for CMC.

Parameter		Value
Input voltage		70.7 V
Input frequency		100 kHz
Output line-to-line voltage		40 V
Output frequency		50 Hz
Carrier frequency		5 kHz
Load	R_{load}	16 Ω
	L_{load}	10 mH

Secondly, the single-phase to three-phase CMC was tested in the experiment with the proposed PDM control methods, which is based on SVM. A high-frequency power source, where the matching impedance is 0 Ω is used as the input of the circuit in this experiment. Table II shows the experimental conditions in order to demonstrate the validity of the proposed PDM methods in CMC in section IV-C.

A. Experimental Results using IMC with PDM Control using Delta-sigma Conversion

Fig. 8(a) shows the operation waveforms of the proposed circuit with delta-sigma conversion. From the result, the output voltage and current are 50-Hz sinusoidal waveforms. The PDM control operation using delta-sigma conversion can be verified and confirmed at the experimental results. Similarly to the simulation

results, certain voltage pulses are inversed due to the failure on the pattern conversion.

Fig. 8(b) shows the extended view of the interval "A" in Fig. 8(a). The results confirm that the switching at zero voltage is approximately performed at the zero cross point of the input voltage waveform. However, the switching has a 1 μs delay due to the following reasons; (i) detection of the zero cross points is slow and (ii) the dead time of the inverter. The delay of the zero cross point detection is approximately 0.5 μs, and dead time of the inverter is set to 0.5 μs. The delay can be improved by modifying the zero cross point detection circuit. Thus, the dead time period can be improved by studying and evaluating the device parameters. Additionally, although the switching has a short delay, the surge voltage is lower than that of the hard switching method. However, due to the clamp phenomena, as covered in the section III-B, switching loss increases because switching at zero voltage cannot be achieved. Therefore, the circuit has low efficiency in this experiment.

In addition, Fig. 9 shows the harmonics analysis on the output voltage and input current. From (a), output voltage does not include low-order harmonic components, and the integral-multiple harmonic nearly closed to 200 kHz. The frequency is DC link voltage fluctuating frequency is included in the high-order harmonic components. The output voltage THD of 5.96% is obtained. Moreover, (b) shows that the input current has the integral-multiple harmonic nearly closed to 100 kHz, and therefore input current THD is 79.7%.

B. Experimental Results using IMC with PDM Control based on Space Vector Modulation

Fig. 10(a) shows the operation waveforms of the proposed circuit in the experiment with the PDM control based on SVM. The result confirms that 50 Hz sinusoidal waveforms are obtained on the output voltage and current. The PDM control operation based on SVM can be verified and confirmed from the experimental results. Notice there are no inverse voltage pulses in this case.

Fig. 10(b) shows the extended view of the interval "B" in Fig. 10(a). As a result, the output line-line voltage v_{uv} confirms that the switching of the inverter is happened at approximately each zero cross point of the 100 kHz sinusoidal input waveform. However, the switching has a 1 μs delay due to the same reasons as mentioned in the explanation of Fig. 8.

Fig. 11 shows the harmonics analysis on the output voltage from experimental result with the PDM control based on SVM. From the result, the low-order harmonic components closely to 50 Hz are not included in the output voltage, and the output voltage THD of 2.15% can be obtained. Therefore, the improvement of the output voltage waveform is confirmed. In this case, output voltage includes of the integral-multiple harmonic nearly to the carrier frequency of 5 kHz, which is the switching frequency. Additionally, the integral-multiple harmonic nearly to the 200 kHz is included in the output voltage

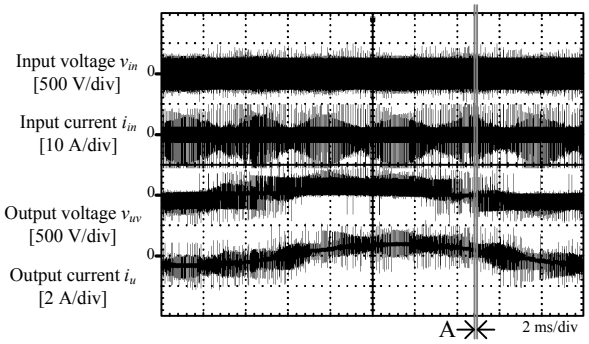

(a) Input and output operation waveforms.

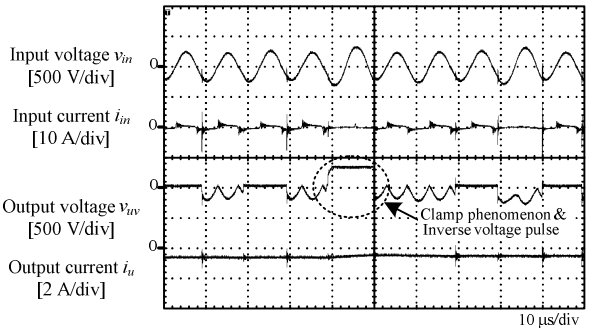

(b) Extended view of each operation waveform.

Fig. 8. Operation waveforms of the proposed circuit in the experiment with PDM using delta-sigma conversion in IMC.

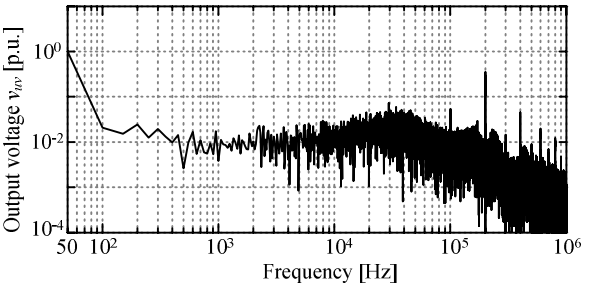

(a) Harmonics analysis of output voltage.

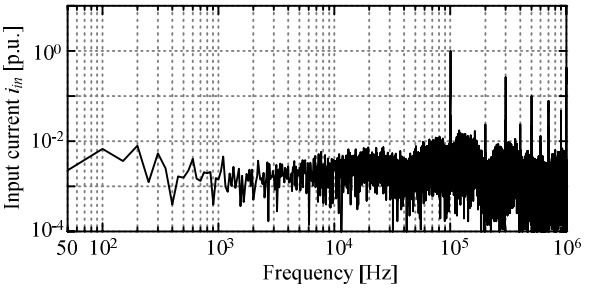

(b) Harmonics analysis of input current.

Fig. 9. Harmonics analysis of output voltage and input current with PDM control using delta-sigma conversion in IMC.

because of the same reason as case of Fig. 9. Furthermore, input current includes the integral-multiple harmonic nearly closed to 100 kHz and input current THD is 55.5%.

From these results, the validity of the proposed PDM control for waveform improvement is confirmed. Therefore, in next chapter, the proposed PDM control method is applied to CMC (direct type circuit) in order to check the basic operation of the PDM control in a direct

type circuit.

C. *Experimental Results using CMC with PDM Control based on Space Vector Modulation at low voltage condition*

Fig. 12(a) shows the operation waveforms of the proposed circuit in the experiment with PDM control based on SVM. The result confirms that 50 Hz sinusoidal waveforms are obtained on the output voltage and current. The PDM control operation based on SVM can be verified and confirmed at the experimental results. However, the output waveform has a surge voltage because of the switching delay due to the zero cross point detection circuit.

Fig. 12(b) shows the extended view of the interval "C" in Fig. 12(a). As a result, the output line-to-line voltage v_{uv} confirms that the switching of the CMC is happened at approximately each zero cross point of the 100 kHz sinusoidal input waveform. Therefore, basic operation of the proposed PDM control based on SVM is confirmed.

Fig. 13(a) shows the harmonics analysis on the output voltage from experimental result with PDM control based on SVM. From the result, the low-order harmonic components of 50 Hz are not included in the output voltage, and the output voltage THD of 3.25% can be obtained. In addition, the output voltage includes the integral-multiple harmonic nearly to the carrier frequency of 5 kHz, which is the control cycle. Additionally, the integral-multiple harmonic nearly to the 200 kHz is included in the output voltage in the high-order harmonic components because the output voltage has the fluctuation, which is twice of the input frequency.

Furthermore, Fig. 13(b) shows the harmonics analysis on the input current. From the result, the input current includes the integral-multiple harmonic nearly closed to 100 kHz and the input current THD is 48.5%, which is large value. However, the harmonics can be eliminated by using small input filter with small capacitor because the cutoff frequency can be very high frequency.

Therefore, the basic operation of the proposed PDM control method in direct type circuit is confirmed from these results.

V. Efficiency Characterristics and Loss Analysis

Fig. 14 shows the efficiency characteristics of the indirect type circuit (IMC) with PDM control using delta-sigma conversion and PDM control based on SVM. The input and output voltage conditions are same as shown in table 1, and the output power is controlled by changing the load value. From the result, the efficiency of the circuit is improved as output power increases in both the PDM control methods. Furthermore, the efficiency for the PDM control based on SVM is higher than that for the PDM control using delta-sigma conversion at all measurement regions. This is because the switching loss decreases due to resolution of the clamp phenomenon and reduction of the switching frequency applying the PDM

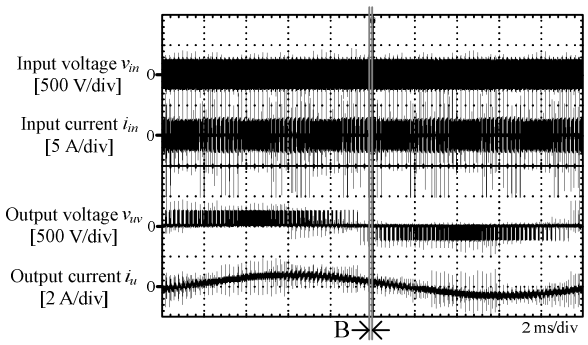

(a) Input and output operation waveforms.

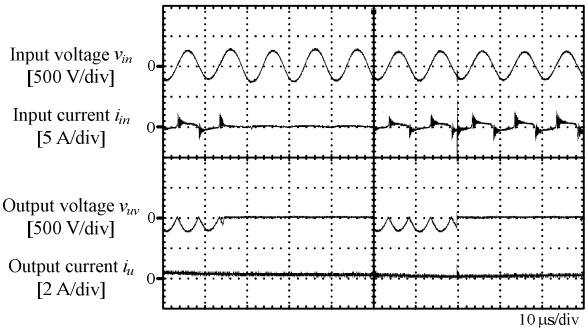

(b) Extended view of each operation waveform.

Fig. 10. Operation waveforms of the proposed circuit in the experiment based on SVM in IMC.

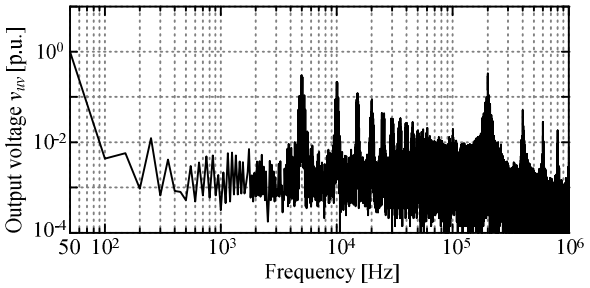

(a) Harmonics analysis of output voltage.

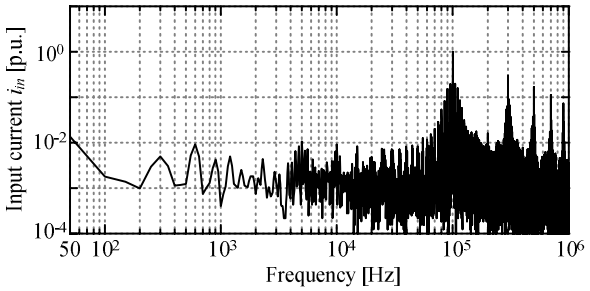

(b) Harmonics analysis of input current.

Fig. 11. Harmonics analysis of output voltage and input current with PDM control based on SVM in IMC.

control based on SVM. As a result, the validity of PDM control based on SVM is confirmed about efficiency improvement.

In addition, the maximum efficiency with PDM control using delta-sigma conversion and with PDM control based on SVM are 93.4% and 97.3% respectively.

Fig. 15 shows the efficiency characteristics of the direct type circuit (CMC) with PDM control based on SVM. The input and output voltage conditions are same

as shown in table II, and the output power is controlled by changing the load value as the case of IMC. From the result, the maximum efficiency is 91.5% at load of 35 W. This value is lower than that of IMC. The cause of low efficiency in the CMC circuit is investigated from the result of the loss analysis.

Fig. 16 shows the result of the loss analysis. From the results, it is confirmed that the cause of low efficiency in the CMC circuit is the conduction loss of the switching device is larger than that of IMC. In this experiment, the current value, which flows through switching devices is larger than case of IMC to output same power because the input and output voltage of the circuit is lower than the case of IMC. It is a limitation of the voltage source, which is used in this experiment. In addition, the bidirectional switches have high on-resistance because the bidirectional switches used in CMC construct of two unidirectional switching devices connected in anti-series.

Therefore, the efficiency of IMC improves by making an experiment at high voltage condition and choosing the switching devices, which have lower on-resistance.

It is noted that the recovery losses of the freewheeling diodes (FWD) and diode rectifier are not included in this simulation. Thus the value of the total loss is lower than actual value.

VI. CONCLUSIONS

In this paper, the implementation of PDM control methods in a single-phase to three-phase matrix converter for high frequency application is discussed and evaluated by the experiments. In the PDM control using delta-sigma conversion, the output waveform has inverse voltage pulse and clamp phenomena on the output voltage waveform. Hence, an improvement method of the output waveform based on SVM is proposed. In SVM, the phase error between the voltage and current are dramatically reduced.

At first a prototype of indirect type circuit has been built and tested. From the results, the switching at zero voltage and clear sinusoidal output waveform have been confirmed. On the other hand, it is confirmed that the PDM control based on SVM can resolve the problems with clamp phenomenon. As a result, the THD of the output voltage with delta-sigma conversion and PDM pattern method based on SVM are 5.96% and 2.15% respectively. Furthermore, the maximum efficiency has been improved from 93.4% to 97.3% by applying the proposed PDM method. From the results, the validity of PDM control based on SVM has been confirmed.

Secondly, a prototype of direct type circuit was built and tested. From the results, the switching at zero voltage and clear sinusoidal output waveform have been confirmed too. As a result, the output voltage THD and input current THD, which is controlled by the proposed PDM based on SVM are 3.25% and 48.5%, respectively.

In addition, the AC-to-AC converter for the high-frequency application such as the proposed circuit is necessary in other case. For example, the MC for high-frequency application can be applied to trans-linked converter, whose secondary side is connected to commercial grid. For downsizing the converter, the transformer for high-frequency link size is a major bottleneck [14]. Therefore, the size of the transformer can be small by higher frequency converter using high-speed switching devices such as SiC and GaN.

In future work, efficiency characteristics of the proposed circuit will be measured, and the zero cross

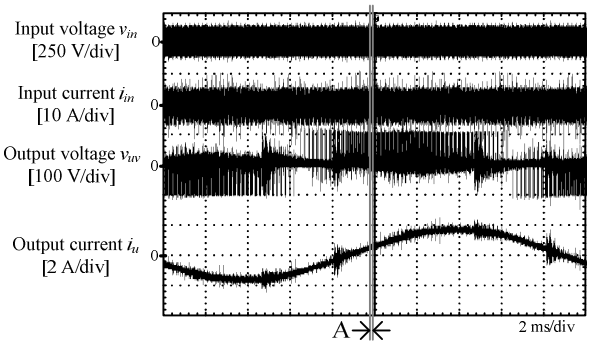

(a) Input and output operation waveforms.

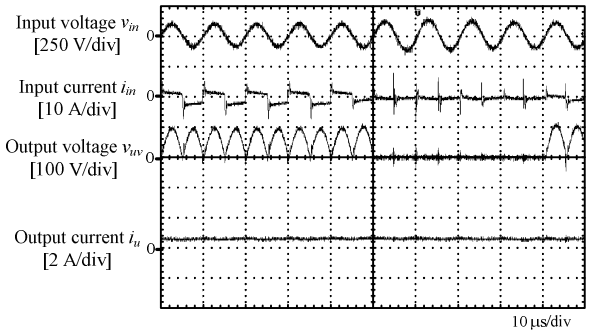

(b) Extended each operation waveform.

Fig. 12. Operation waveforms of the proposed circuit in the experiment based on SVM in CMC.

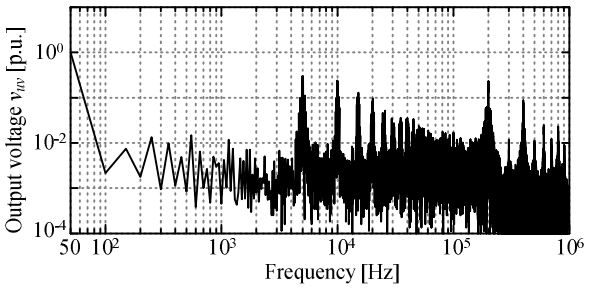

(a) Harmonics analysis of output voltage.

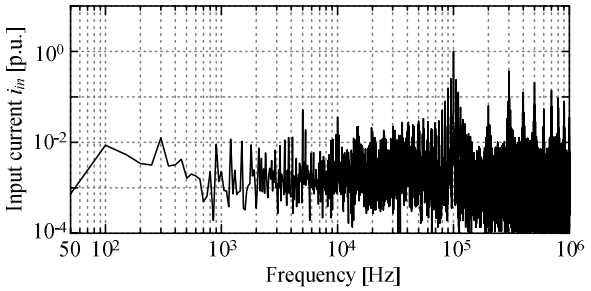

(b) Harmonics analysis of input current.

Fig. 13. Harmonics analysis of output voltage and input current with PDM control based on SVM in CMC.

point detection circuit will be improved to reduce the switching loss and the switching surge.

REFERENCES

[1] Takehiro IMURA, Yoichi HORI : "Wireless power transfer using electromagnetic resonant coupling", The Journal of The Institute of Electrical Engineers of Japan, vol.129, No.7 pp.414-417, July 2009 (in Japanese)

[2] Keisuke Kusaka and Jun-ichi Itoh, "Experimental verification of rectifiers with SiC/GaN for wireless power transfer using a magnetic resonance coupling", The 9th IEEE International Conference on Power Electronics and Drive Systems, pp. 1094-1099, December 2011

[3] Keisuke Kusaka, Satoshi Miyawaki and Jun-ichi Itoh : "A experimental evaluation of a SiC schottky barrier rectifier with a magnetic resonant coupling for contactless power transfer as a power supply", 2010 Annual Conference of IEEJ, Industry Applications Society, No.1-41, 2010 (in Japanese)

[4] A.Kurs, A. Karalis, R. Moffatt, J. D. Joannopoulos, P. Fisher and M. Soljačić, "Wireless power transfer via strongly coupled magnetic resonances", Science, vol.317, pp.83-86, June 2007

[5] Patrick W. Wheeler, José Rodríguez, Jon C. Clare, Lee Empringham and Alejandro Weinstein, "Matrix converters : A technology review", IEEE Transactions on Industry Electronics, Vol. 49, No. 2, pp.274-288, April 2002

[6] Yugo Tadano, Shizunori Hamada, Shota Urushibata, Masakatsu Nomura, Yukihiko Sato and Muneaki Ishida, "A space vector modulation scheme for matrix converter that gives top priority to the improvement of the output control performance", IEEJ Transactions on Industry Applications, Vol.128, No.5, pp.631-641, May 2008 (in Japanese)

[7] Jun-ichi Itoh, Ikuya Sato, Hideki Ohguchi, Kazuhisa Sato, Akihiro Odaka and Naoya Eguchi, "A control method for the matrix converter based on virtual AC/DC/AC conversion using carrier comparison method", IEEJ Transactions on Industry Applications, vol.124, No.5, pp.457-463, May 2004 (in Japanese)

[8] Y. L. Feng, Y. Konishi, M. Nakaoka, "Current-fed soft-switching inverter with PDM-PWM control scheme for ozone generation tube drive", IEEJ Transactions on Industry Applications, Vol.120, No.10 pp.1239-1240, October 2000 (in Japanese)

[9] P.K.Sood and T.A.Lipo : "Power Conversion Distribution System using a High-Frequency AC Link," IEEE Trans. on IA, Vol.IA-24, No.2, pp.228-300 (1988)

[10] Hisayuki Sugimura, Bishwajit Saha, H. Omori, Hyun-Woo Lee, M. Nakaoka, "Single reverse blocking switch type pulse density modulation controlled ZVS inverter with boost transformer for dielectric barrier discharge lamp dimmer", IEEE 5th International Power Electronics and Motion Control Conference, 2006, vol. 2, pp. 1 - 5, August 2006

[11] Abdelhalim Sandali, Ahmed Cheriti and Pierre Sicard, "Design considerations for PDM Ac/ac converter implementation", Applied Power Electronics Conference 2007, pp. 1678 - 1683, February 2007

[12] Yuki Nakata and Jun-ichi Itoh, "An experimental verification and analysis of a single-phase to three-phase matrix converter using PDM control method for high-frequency applications", The 9th IEEE International Conference on Power Electronics and Drive Systems, No. 383, pp.1084-1089, December 2011

[13] Yuki Nakata and Jun-ichi Itoh, "Control methods of an indirect-type Single-phase to three-phase matrix converter for high-frequency applications", Workshop on Semiconductor Power Converter, SPC-12-029, January 2012 (in Japanese)

[14] Masayoshi Yamamoto, Hiroyuki Horii, "Trans-linked single phase interleaved PFC converter", IEEJ Transactions on Industry Applications, Vol.130, No.6, pp.828-829, June 2010 (in Japanese)

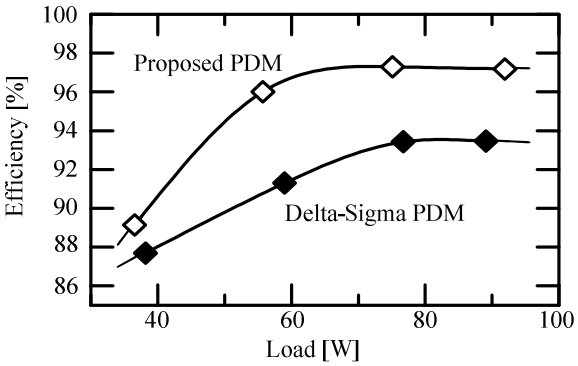

Fig. 14. Characteristics of the proposed circuit's efficiency in the experiment using IMC.

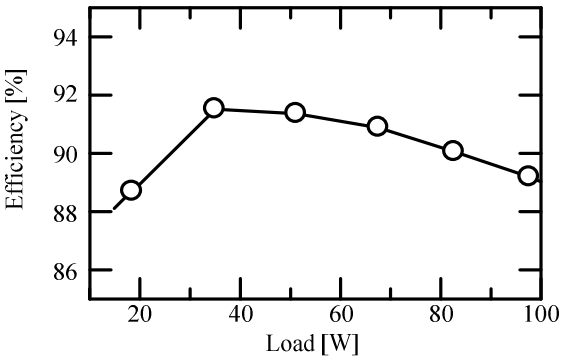

Fig. 15. Characteristics of the proposed circuit's efficiency in the experiment using CMC.

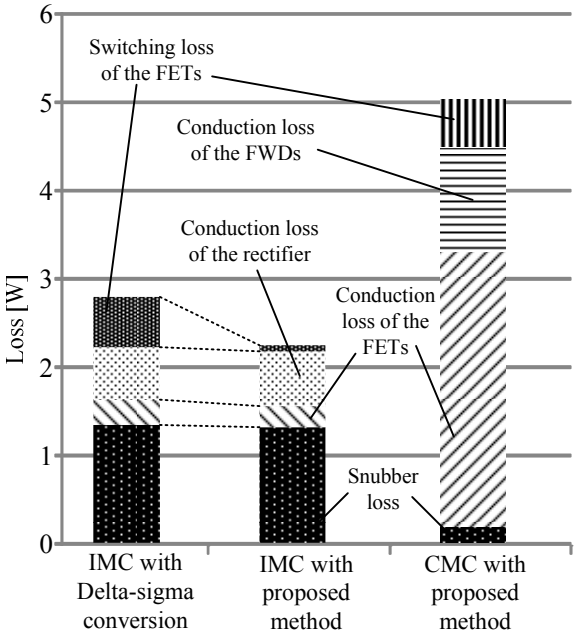

Fig. 16. Loss analysis of the IMC and the CMC with 100-W load.